Inorg. Chem. **2008**, *47*, 5184−5189

^{67}Zn Solid-State NMR Spectroscopy of {[Tp^{But,Me}]Zn(OH$_2$)}[HOB(C$_6$F$_5$)$_3$]. The Importance of the Anion [HOB(C$_6$F$_5$)$_3$]$^-$

Andrew S. Lipton,[†] Melissa M. Morlok, Gerard Parkin,*[,‡] and Paul D. Ellis*[,†]

Biological Sciences Division, Pacific Northwest National Laboratories, 902 Battelle Boulevard, Richland, Washington 99352, and Department of Chemistry, Columbia University, 3000 Broadway, New York, New York 10027

Received January 2, 2008

One of the paradigms of Zn^{2+} metallobiochemistry is that coordination of water to Zn^{2+} provides a mechanism of activation that involves lowering the pK_a by approximately 7 pH units. This idea has become central to the development of mechanisms of action for zinc metalloproteins. However, the direct measurement of the pK_a of water bound to Zn^{2+} in a metalloprotein has yet to be accomplished. Developing models for Zn^{2+}−OH_2 species has been a significant challenge, but we have utilized solid-state ^{67}Zn NMR spectroscopy as a means to characterize one of the few examples of water bound to mononuclear tetrahedral Zn^{2+}: {[Tp^{But,Me}]Zn(OH$_2$)}[HOB(C$_6$F$_5$)$_3$]. The measured quadrupole coupling (C_q) constant is 4.3 MHz with an asymmetry parameter of η_q of 0.6. Likewise, due to the small value of C_q, anisotropic shielding also contributed to the observed ^{67}Zn NMR lineshape. As expected, the computed values of the magnetic resonance parameters depend critically on the nature of the anion. The predicted value of C_q for {[Tp^{But,Me}]Zn(OH$_2$)}[HOB(C$_6$F$_5$)$_3$] is −4.88 MHz. We discuss the results of these calculations in terms of the nature of the anion, the local electrostatics, and its subsequent hydrogen bonding to [Tp^{But,Me}]Zn(OH$_2$)$^+$.

Introduction

One of the principal paradigms of Zn^{2+} metallobiochemistry is that coordination of H_2O to Zn^{2+} facilitates deprotonation at close to neutral pH. The classic example is provided by carbonic anhydrase (CA) for which the mechanism of the reaction was proposed to involve conversion to a zinc-bound hydroxide followed by attack at CO_2.[1] Examination of the pH dependence of k_{cat} bolstered the assumption, with the resulting sigmoidal plot having all of the features of an acid/base titration curve, the midpoint being the pK_a of a group critical for protein activity.[2,3] Whereas this behavior has been interpreted to be a result of the ionization of a metal-bound water molecule,[4] our recent work suggests that this assumption might not be the case.[5]

Such an assumption is difficult to model using simple inorganic compounds. The major difficulty comes from the charged nature of the active site in the protein. For example, the active metal site in CA is thought to be either [(His)$_3$ZnOH]$^{1+}$ for the hydroxide form or [(His)$_3$ZnOH$_2$]$^{2+}$ for the aqua form, with the remainder of the protein serving as the anion. However, the synthetic inorganic chemist does not have the luxury of having such a charge buffer. Rather, there must be a discrete anion to balance the charge of the cation. The nature of that anion is critical to the stability and functionality of the overall complex. Recently, this synthetic challenge has been the focus of several reports.[6–10] Of particular interest to us here is the tris(pyrazoyl)hydroborato complex {[Tp^{But,Me}]Zn(OH$_2$)}[HOB(C$_6$F$_5$)$_3$] (**I**) (Figure 1)[6,7] because of the close structural resemblance to

* To whom correspondence should be addressed. E-mail: parkin@columbia.edu (G.P.), paul.ellis@pnl.gov (P.D.E.). Phone: 509 371 6550. Fax: 509 371 6555.
† Pacific Northwest National Laboratories.
‡ Columbia University.

(1) Christianson, D. W.; Fierke, C. A. *Acc. Chem. Res.* **1996**, *29*, 331–339.
(2) Cook, P. F.; Cleland, W. W. *Enzyme Kinetics and Mechanism*; Garland Science: London and New York, 2007.
(3) Coleman, J. E.; Gettins, P. *Molecular Properties and Mechanism of Alkaline Phosphatase*; John Wiley & Sons: New York, 1983; Vol. *5*.
(4) Kiefer, L. L.; Fierke, C. A. *Biochemistry* **1994**, *33*, 15233–15240.
(5) Lipton, A. S.; Heck, R. W.; Ellis, P. D. *J. Am. Chem. Soc.* **2004**, *126*, 4735–4739.
(6) Bergquist, C.; Parkin, G. *J. Am. Chem. Soc.* **1999**, *121*, 6322–6323.
(7) Bergquist, C.; Fillebeen, T.; Morlok, M. M.; Parkin, G. *J. Am. Chem. Soc.* **2003**, *125*, 6189–6199.
(8) Voo, J. K.; Incarvito, C. D.; Yap, G. P. A.; Rheingold, A. L.; Riordan, C. G *Polyhedron* **2004**, *23*, 405–412.
(9) Voo, J. K.; Incarvito, C. D.; Yap, G. P. A.; Rheingold, A. L.; Riordan, C. G *Polyhedron* **2006**, *25*, 1873.
(10) Parkin, G. *Chem. Rev.* **2004**, *104*, 699–767.

10.1021/ic800009b CCC: $40.75
Published on Web 05/10/2008

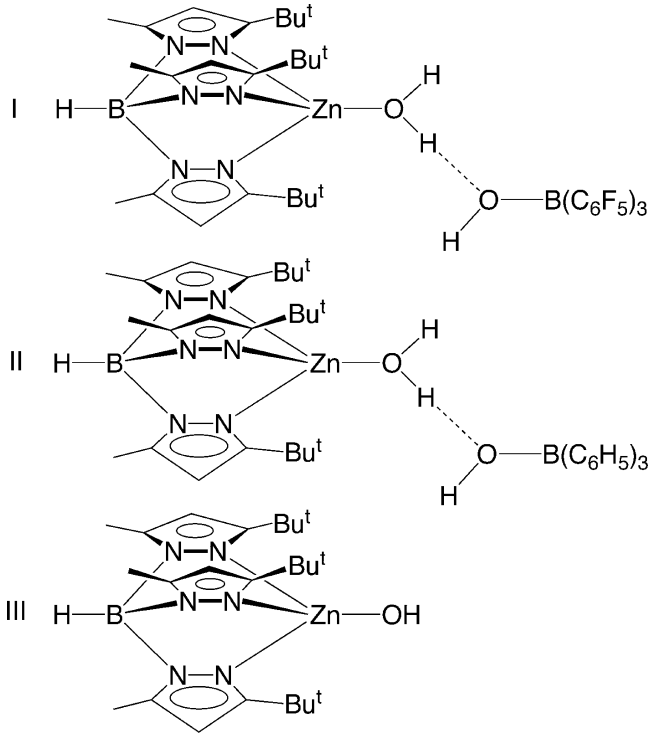

Figure 1. {[Tp^{But,Me}]Zn(OH$_2$)}[HOB(C$_6$F$_5$)$_3$] (**I**), {[Tp^{But,Me}]Zn(OH$_2$)}-[HOB(C$_6$H$_5$)$_3$] (**II**) and {[Tp^{But,Me}]ZnOH (**III**).

[(Im)$_3$ZnOH$_2$]$^{2+}$ (where the abbreviation "Im" is used to denote the imidazole portion of the histidine ligand bound to the Zn^{2+}), although there are some important differences. For example: (i) in CA, two of the histidines coordinate through their ε-nitrogens, whereas one coordinates through its δ-nitrogen, and (ii) the charge associated with the aqua species {[Tp^{But,Me}]Zn(OH$_2$)}$^+$ is +1 for **I**, whereas it is +2 for the aqua form of CA [(Im)$_3$ZnOH$_2$]$^{2+}$.

It is important to note that the pK_a of water bound to zinc has yet to be measured directly in *any* protein. Describing the ionization of a zinc-bound water by a simple pK_a makes the assumption that zinc-bound water at the active site of a protein can be described as a simple weak acid. Such an assumption ignores the possible complexity introduced by hydrogen bonding at the active site and the nature of other ionizable functionalities, which could be hydrogen bonded to the water.

The difference in the bond distances between water and hydroxide bound to zinc is approximately 0.1 Å,[7,11] a difference that cannot be reliably measured by X-ray diffraction studies on proteins. Furthermore, at or near the pK_a of the system, the resulting crystal would be disordered, that is, composed of a random mixture of Zn−OH and Zn−OH$_2$ moieties, in such a manner that the hydroxide and aqua sites cannot be resolved by X-ray diffraction. Recently, we developed a spectroscopic method utilizing solid-state ^{67}Zn NMR spectroscopy that would be capable of a measurement of the relative amounts of zinc-bound water and hydroxide.[5,12] Using these methods, we report here the characterization of **I** by ^{67}Zn NMR spectroscopy. Additionally, by using standard electronic structure methods, we examine the importance of the anion by contrasting the prediction of the observed C_q for **I** with that for the theoretical construct {[Tp^{But,Me}]Zn(OH$_2$)}[HOB(C$_6$H$_5$)$_3$] (**II**), in which the fluorine atoms have been replaced by hydrogen atoms.

Experimental Methods

Preparation of Co^{2+}-Doped {[Tp^{But,Me}]Zn(OH$_2$)}[HOB(C$_6$F$_5$)$_3$]. All manipulations were performed under a N_2 atmosphere employing standard Schlenk and glovebox techniques. {[Tp^{But,Me}]Zn-(OH$_2$)}[HOB(C$_6$F$_5$)$_3$] and {[Tp^{But,Me}]Co(OH$_2$)}[HOB(C$_6$F$_5$)$_3$] were prepared as previously reported.[7] Samples of {[Tp^{But,Me}]Zn-(OH$_2$)}[HOB(C$_6$F$_5$)$_3$] doped with ca. 2% by weight of {[Tp^{But,Me}]Co(OH$_2$)}[HOB(C$_6$F$_5$)$_3$] were prepared by a sequence involving dissolving the mixture in benzene, followed by lyophilization to remove the benzene.

NMR Measurements. All zinc chemical shifts are referenced with respect to 1 M Zn(NO$_3$)$_{2(aq)}$ (measured at ambient temperature). The ^{67}Zn powder spectrum acquired at 21.15 T was obtained at ambient temperature utilizing a Varian Unity^{Inova} spectrometer with a medium-bore (63 mm) Oxford Instruments magnet operating at 21 T (900 MHz for ^{1}H and 56.316 MHz for ^{67}Zn) and a home-built 5 mm wide-line probe. The cryogenic (10 K) data was obtained on a Varian Unity^{Inova} spectrometer with a medium-bore (63 mm) Oxford Instruments magnet operating at 18.8 T (800 MHz for ^{1}H and 50.048 MHz for ^{67}Zn) and a Varian Infinity^{Plus} spectrometer with a wide-bore (89 mm) Oxford Instruments magnet operating at 9.4 T (400 MHz for ^{1}H and 25.035 MHz for ^{67}Zn) with an Oxford Instruments continuous flow cryostat for each system. The cryostat is top-loaded into the bore of the magnet, and a home-built NMR probe is then inserted into the sample space of the cryostat.[13,14]

The pulse sequences used were a combination of cross polarization (CP)[15] with signal detection using either a single Hahn echo or a quadrupole Carr−Purcell−Meiboom−Gill (QCPMG) echo train.[16,17] The spectra acquired at the lower field required a stepped offset frequency and reconstruction using a sky projection.[18] The chosen offsets were 10 kHz steps made relative to the 0.0 ppm shift of 1 M Zn(NO$_3$)$_2$. The resulting spectra were analyzed using the *SIMPSON* program.[19] Simulations of the NMR spectra were performed on a Beowulf cluster at PNNL (composed of a 40-Verari Dual Socket, Dual Core Intel 5140 2.33 GHz Xeon nodes, 24-Racksaver[20] Dual Pentium IV 2.4 GHz Xeon nodes, and 6-Racksaver Dual Pentium III 1.26 GHz nodes) running the *Rocks* clustering software and utilizing a gigabit Ethernet connection.

Computation Details. Calculations were performed using the program *NWChem*.[21,22] A key feature of the present work is the

(11) Alsfasser, R.; Trofimenko, S.; Looney, A.; Parkin, G.; Vahrenkamp, H. *Inorg. Chem.* **1991**, *30*, 4098–4100.
(12) Ellis, P. D.; Lipton, A. S *Annu. Rep. NMR Spectrosc.* **2007**, *60*, 1–38.
(13) Lipton, A. S.; Sears, J. A.; Ellis, P. D. *J. Magn. Reson.* **2001**, *151*, 48–59.
(14) Lipton, A. S.; Heck, R. W.; Sears, J. A.; Ellis, P. D. *J. Magn. Reson.* **2004**, *168*, 66–74.
(15) Pines, A.; Gibby, M. G.; Waugh, J. S *J. Chem. Phys.* **1972**, *56*, 1776.
(16) Larsen, F. H.; Jakobsen, H. J.; Ellis, P. D.; Nielsen, N. C. *J. Phys. Chem. A* **1997**, *101*, 8597–8606.
(17) Larsen, F. H.; Lipton, A. S.; Jakobsen, H. J.; Nielsen, N. C.; Ellis, P. D. *J. Am. Chem. Soc.* **1999**, *121*, 3783–3784.
(18) Lipton, A. S.; Wright, T. A.; Bowman, M. K.; Reger, D. L.; Ellis, P. D. *J. Am. Chem. Soc.* **2002**, *124*, 5850–5860.
(19) Bak, M.; Rasmussen, J. T.; Nielsen, N. C. *J. Magn. Reson.* **2000**, *147*, 296–330.
(20) Racksaver is now Verari Systems.
(21) Aprà, E.; et al. *NWChem, A Computational Chemistry Package for Parallel Computers, ver. 5.0]*; Pacific Northwest National Laboratory: Richland, WA, 2004.

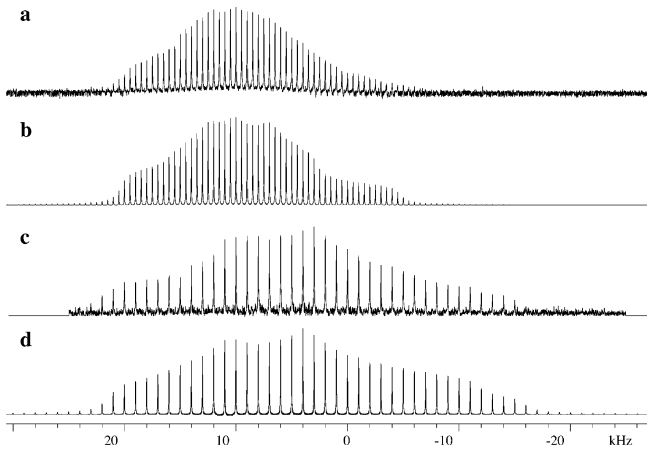

Figure 2. Field dependence of **I** at 18.8 and 9.4 T obtained at 10 K. Panel **a** denotes the data acquired with 256 accumulations obtained at 18.8 T data, and the *SIMPSON* fit of this is illustrated in panel **b**. Panel **c** illustrates the experimental data obtained at 9.4 T acquired with 2048 acquisitions, and the corresponding *SIMPSON* fit is shown in panel **d**.

comparison of the computed predictions between **I** and the theoretical construct **II**. Because a crystal structure for **II** is not available, it is more appropriate to compare only the results of gas-phase calculations rather than utilize a solid-state calculation for **I** and a gas-phase calculation for **II**. Hence, *all*of the calculations were performed in the gas phase. All geometry optimizations utilized Ahlrich's double-ζ level (including polarization functions) basis set (pAVDZ);[23] utilizing this geometry, subsequent property calculations (the electric-field gradient and shielding tensors at the Zn^{2+}) utilized Ahlrich's triple-ζ basis set including polarization functions (pATZV).[24] The Ahlrich's basis sets have provided excellent results from prior investigations, hence, their use in the present study.[25,26] These basis sets (including added polarizations' functions) are available for download from the Environmental Molecular Sciences Laboratory (EMSL) using a basis set order form or as part of the Extensible Computational Chemistry Environment (ECCE) software package.[27,28] All of the calculations were performed using rhf methods. The calculations were carried out on the Beowulf cluster mentioned above using either the Xeon or P4 nodes.

Results and Discussion

Zinc is a quadrupolar nuclide with a spin quantum number I of $^5/_2$. The NMR lineshape associated with such a nuclide is typically dominated by the so-called central transition (CT).[29] The principal observable that can be extracted from the CT is the quadrupole coupling constant, C_q. This coupling constant is directly proportional to the electric-field gradient at the nuclide and is given by

$$C_q = q_{zz}\left[\frac{e^2}{a_0^3 h}\right]Q \tag{1}$$

$$= q_{zz}\,35.24474\ \text{MHz} \tag{2}$$

Here, Q is the quadrupole moment of the nucleus in question, and q_{zz} is defined as the largest absolute value of the computed field gradient tensor in the principal axis system (PAS) described by diagonalized field gradient tensor q. The traceless field gradient tensor[29] in its PAS frame can be described in terms of q_{zz} and its asymmetry parameter, η_q, where

$$|q_{zz}| \geq |q_{yy}| \geq |q_{xx}| \quad \eta_q \equiv \frac{q_{xx} - q_{yy}}{q_{zz}} \tag{3}$$

The units for q_{zz} are atomic units, and the factor of 35.24474 MHz can be computed if the atomic constants are expressed in cgs units and the value of Q is given as 0.15×10^{-24} cm^2.[30] The computed value of C_q should be reduced to the correct number of significant figures after the multiplication is carried out. The CT lineshape has a well-defined magnetic field dependence. That is, if the CT lineshape is dominated by a second-order quadrupole interaction, then the breadth of the lineshape, ω, should be proportional to the following factors:

$$\omega \propto \frac{C_q^2}{\omega_0[I(2I-1)]^2} \tag{4}$$

Thus, the breadth of the NMR lineshape is proportional to the square of C_q and inversely proportional to the Larmor frequency, ω_0, of the nucleus in question and its spin quantum number. This field dependence becomes an essential tool in the disentanglement of quadrupolar lineshapes. A detailed analysis of the experimental lineshape yields C_q, which in turn affords the determination of the field gradient at Zn^{2+}.

Figure 2 illustrates the ^{67}Zn NMR spectrum of **I** at two magnetic field strengths (9.4 and 18.8 T) at cryogenic temperatures (10 K). Figure 3 shows the data acquired for **I** at ambient temperature at 21.15 T. The spectra, on a relative scale, are narrow; the spectrum at 9.4 T being the broadest is a modest 40 kHz wide. A close examination of the two figures illustrates that the spectra at the three fields are different. The dominant difference that is observed in these lineshapes at the various fields reflects the expected inverse field dependence plus an additional contribution from anisotropic shielding. The presence of anisotropic shielding introduces a field dependence that increases linearly as the field strength increases. This can be seen from an examination of Figure 2. If the ^{67}Zn NMR lineshape were dominated

(22) Kendall, R. A.; Aprà, E.; Bernholdt, D. E.; Bylaska, E. J.; Dupuis, M.; Fann, G. I.; Harrison, R. J.; Ju, J.; Nichols, J. A.; Nieplocha, J.; Straatsma, T. P.; Windus, T. L.; Wong, A. T. *Comput. Phys. Commun.* **2000**, *128*, 260–283.
(23) Schafer, A.; Horn, H.; Ahlrichs, R. *J. Chem. Phys.* **1992**, *97*, 2571–2577.
(24) Schafer, A.; Huber, C.; Ahlrichs, R. *J. Chem. Phys.* **1994**, *100*, 5829–5835.
(25) Lipton, A. S.; Bergquist, C.; Parkin, G.; Ellis, P. D. *J. Am. Chem. Soc.* **2003**, *125*, 3768–3772.
(26) Lipton, A. S.; Ellis, P. D *J. Am. Chem. Soc.* **2007**, *129*, 9192–9200.
(27) http://www.emsl.pnl.gov/forms/basisform.html.
(28) Basis sets were obtained from the Extensible Computational Chemistry Environment Basis Set Database, version 02/25/04, as developed and distributed by the Molecular Science Computing Facility, Environmental and Molecular Sciences Laboratory, which is part of the Pacific Northwest Laboratory, P.O. Box 999, Richland, Washington 99352, U.S.A., and is funded by the U.S. Department of Energy. The Pacific Northwest Laboratory is a multiprogram laboratory operated by Battelle Memorial Institute for the U.S. Department of Energy under Contract DE-AC06–76RLO 1830. Contact Karen Schuchardt for further information.
(29) Cohen, M. H.; Reif, M. G. *Solid State Phys.* **1957**, 5.
(30) Pyykko, P. *Mol. Phys.* **2001**, *99*, 1617–1629.

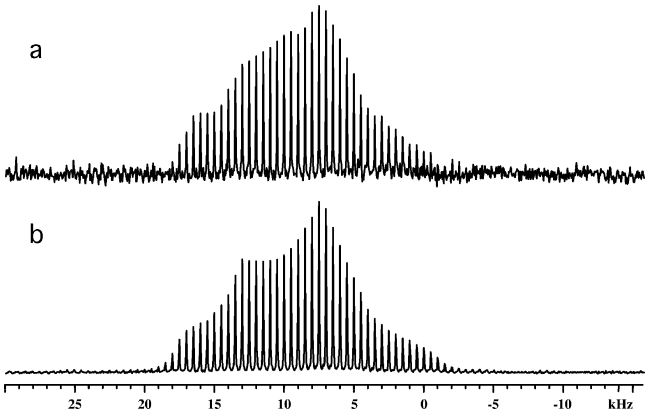

Figure 3. Panel **a** illustrates the data acquired at 21.15 T with 65 536 acquisitions, whereas panel **b** shows the corresponding *SIMPSON* fit to the data.

Table 1. Experimental and Predicted NMR Parameters

	theory		experimental
	I	**II**	**I**
C_q[a]	−4.88	29.79	4.3 (3.6)[b]
η_q	0.39	0.18	0.6 (0.6)
$\Delta\sigma$[c]	166.81	324.43	−256.5 (177.0)
η_{cs}	0.42	0.15	0.6 (0.7)
α[d]	87		134 (129)
β[d]	108		75 (65)
γ[d]	157		34 (148)

[a] C_q values are in MHz; the computed sign cannot be determined experimentally from the data presented here. [b] The values in parentheses were determined at room temperature at 21.15 T. The other values were extracted from data obtained at 10 K and 18.8 T. [c] σ_{iso} denotes the trace of the matrix σ, using the following ordering $|\sigma_{33} - \sigma_{iso}| \geq |\sigma_{11} - \sigma_{iso}| \geq |\sigma_{22} - \sigma_{iso}|$; the anisotropy and asymmetry parameter are defined as $\Delta\sigma = \sigma_{33} - \frac{1}{2}(\sigma_{11} + \sigma_{22})$, $\eta_{cs} = (\sigma_{22} - \sigma_{11})/(\sigma_{33} - \sigma_{iso})$. The units are ppm; the relative uncertainty in anisotropy is ±0.5 ppm. The uncertainty in the respective asymmetry parameters is ± 0.1. [d] The angles are in degrees and represent the relative orientation of the shielding tensor with respect to the quadrupole principal axis frame. The relative uncertainty in these numbers is ±5°.

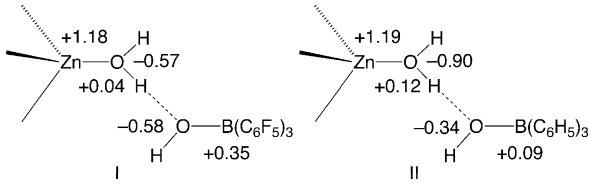

Figure 4. The net charges resulting from a Mulliken charge analysis for the fragment of Zn−O−H···O−B within **I** and **II**.

Table 2. Selected Bond Distances in **I**. Comparison between Theory and Experiment[a]

distance	experiment	theory	difference
Zn_1-O_2	1.937	1.986	0.049
O_1-H_3	1.084	1.000	−0.084
H_3-O_4	1.395	1.543	0.140
O_4-B_5	1.502	1.487	0.015

[a] The numbering system corresponds to the molecular fragment described within the text. All distances are in angstroms.

by the second-order quadrupole interaction, the lineshape obtained at 18.8 T would have half the width of that obtained at 9.4 T. Clearly, that is not the case. The combination of the two interactions (quadrupole and anisotropic shielding) introduces a field dependence to the observed NMR lineshape that depends upon which interaction is dominant. The level of the fit of the experimental data shown in Figure 3, although good, illustrates how difficult it can be to fit the Euler angles relating the relative orientation of the quadrupole and shielding tensors. Analysis of these lineshapes yields not only the field gradient tensor but also the shielding tensor for the $Zn^{2+}$and the relative orientation of the two tensors. The combination of these two molecular parameters provides important constraints for ab initio electronic structure calculations.

The magnetic resonance parameters at the two temperatures are summarized in Table 1. Analysis of the data at *all* field strengths should yield a single set of values for the magnetic resonance parameters for the Zn^{2+} in **I**. However, it appears that the room-temperature spectra yield slightly different values for the parameters when compared to the values obtained at 10 K, that is, Table 1. To a certain extent this is to be expected. Whether this small difference could be described as a phase change, or simply a normal change in unit cell parameters as the temperature is reduced, or an onset of some molecular motion, which gives rise to a partial averaging of the quadrupole and shielding tensors, is unclear.

Analysis of the low-temperature data yielded a quadrupole coupling constant of 4.3 ± 0.1 MHz, with a corresponding asymmetry parameter of 0.6 ± 0.1. Additionally, the low-temperature data were fit simultaneously to provide a determination of the shielding anisotropy at the Zn^{2+}, that is, –256.5 ± 0.5 ppm, with an asymmetry parameter of 0.6 ± 0.1 and the relative orientation of the two tensors. In a previous investigation of the pH dependence of the ^{67}Zn NMR spectroscopy of CA, we utilized a simple computational model for the active site of CA.[5] The models predicted C_q values in the range of 29.2–8.72 MHz for the $[(MeIm)_3Zn-OH]^+$ and 37.6–25.49 MHz for $[(MeIm)_3Zn-OH_2]^{2+}$. The range denoted above arose from different models for the hydrogen bonding to the H_2O, OH^-, and/or the methylimidazoles. The data for **I** is clearly different from the predicted value of C_q for a simple model for $[(MeIm)_3Zn-OH_2]^{2+}$. It is important to note that the charge on this model is +2 and that these calculations were performed in the absence of an anion.

The relatively poor agreement for the predicted value of C_q for **I** and the model for water coordination to Zn^{2+}, $[(MeIm)_3Zn-OH_2]^{2+}$, is to be contrasted to a similar set of calculations used to model OH^- bound to Zn^{2+}.[31] Previously, model calculations for $[(MeIm)_3Zn-OH]^+$ were close to agreement for the synthetic analog $[Tp^{But,Me}]ZnOH$, (**III**),[11] for example the experimental value for **III** was 30.5 MHz, whereas the predicted value was between 28.6 and 34.4 MHz. In this case, the gas-phase calculations on the cation, $[(MeIm)_3Zn-OH]^+$, were close to the experimental value of the neutral compound **III**. Additionally, the presence of hydrogen bonding did not have an appreciable impact on the agreement between theory and experiment. These results suggest that water coordinated to Zn^{2+} requires hydrogen bonding to a greater extent than the corresponding hydroxide.

(31) Lipton, A. S.; Bergquist, C.; Parkin, G.; Ellis, P. D. *J. Am. Chem. Soc.* **2003**, *125*, 3768–3772.

Further, the poor agreement between theory and experiment for the model $[(MeIm)_3Zn-OH_2]^{2+}$ and the present experiment points to the importance of the anion in **I**, the subsequent hydrogen bonding to that anion, and the associated differences in the electrostatics between the cation/anion pair. To examine this assertion, we performed a series of rhf calculations on **I**.

The molecular structure of **I** as determined by X-ray diffraction[7] was used as a starting point for the geometry optimization and subsequent property calculations (the electric field gradient and shielding tensors at the Zn^{2+}), as described above. The results of these calculations are summarized in Table 1. As an illustration of the importance of the anion, we repeated these calculations on the construct **II**. Construct **II** is the same as **I** except that the anion has been changed from $[HOB(C_6F_5)_3]^-$ to $[HOB(C_6H_5)_3]^-$. The predicted magnetic resonance parameters for **I** and **II** are summarized in Table 1. Changing the nature of the anion from **I** to **II** produces a large change in the predicted C_q from –4.88 MHz to +29.79 MHz. Likewise, the predicted changes in the shielding tensor for Zn^{2+} are significant with the shielding anisotropy changes from 166.8 to 324.4 ppm, for **I** and **II**, respectively.

The predicted value of C_q for **I** is in excellent agreement with experiment (at both temperatures). However, the prediction for the shielding anisotropy is relatively poor at low temperature, whereas at ambient temperature the agreement is excellent. The sign change of the anisotropy can occur simply by the interchange of the two shielding tensor elements, that is, σ_{11} and σ_{33}. Whereas we can only speculate as to the origin of these differences, we can only conclude that the agreement between theory and experiment is overall excellent for the room temperature data.

As to be expected, the electrostatics in the vicinity of the hydrogen bond between **I** and **II** are different. Consider the following fragment: $Zn-O-H_3\cdots O-B_5$.

Here, the symbol "$\cdots$" denotes the hydrogen bond in either **I** or **II**. A Mulliken charge analysis on the two complexes yields the following net charges for the atoms from left to right: +1.1786, –0.5696, +0.0402, –0.5828, and +0.3541 for **I** and +1.1924, –0.9047, +0.1196, –0.3414, and +0.0943 for **II**, as illustrated in Figure 4.

Clearly, the largest changes occur in the region of the hydrogen bond. The charge differences at B reflect the nature of the two anions, with $[HOB(C_6F_5)_3]^-$ being more electron withdrawing than $[HOB(C_6H_5)_3]^-$. The $[HOB(C_6F_5)_3]^-$ anion has the further advantage that the hydrogen can stabilize the orientation of one of the C_6F_5 rings through a hydrogen bond with the *meta*-F. This computed distance is 1.979 Å, whereas experimentally the distance is 2.182 Å. The corresponding interaction in **II** is absent and results in a predicted distance between the two atoms of 2.506 Å. The electrostatics change as a result of the change in anions, but the H$\cdots$O distance does not appear overly sensitive to the nature of the charge differences, with the computed hydrogen bond distance changing from 1.543 (**I**) to 1.549 Å (**II**). Hence, although there are only small structural changes associated with the two anions, the quadrupole parameters change dramatically.

Summary and Conclusions

We have extracted the magnetic resonance parameters associated with the Zn^{2+} site for **I**. This complex serves as one of the few models for water coordinated to Zn^{2+} in a metalloprotein, such as CA. The level of agreement between theory and experiment for *both* the quadrupole coupling constant and the anisotropic shielding anisotropy of **I** are excellent. The results of the calculations, as expected, depend critically on the nature of the anion coupled to the cation in **I**. The predicted NMR parameters for **I** have been contrasted to those for construct **II**, and the predicted quadrupole and shielding parameters change significantly, for example the predicted value of C_q changes from –4.88 in **I** to 29.79 in **II**. Whereas the NMR parameters change dramatically, the structural parameters do not. For example, the distance between O$\cdots$H in the hydrogen bond differs only subtly. The value of the quadrupole coupling constant in **I** or **II** appears to be dominated by the electrostatics in vicinity of the hydrogen bond, rather than any particular structural parameter.

If we consider the level of agreement between theory and experiment in the present case as typical, then the combination of molecular theory and low-temperature solid-state NMR spectroscopy of metals at the active site of a metalloprotein can be utilized to develop a model for the active site of the protein. This model would be able to distinguish between OH and water bound to the given active site metal ion. Although typically X-ray structures of proteins do not include the position of the protons, the protons can be added to a crystal structure via standard methods. However, that structure needs to be energy minimized, for example one approach being the utilization of QM/MM methods.[32–35] The resulting quantum region of that structure represents the model for the active site of the protein. For this model to be of value, it should be able to predict various ground-state molecular parameters, such as bond distances, angles, and magnetic resonance parameters. In our case, we can compare quadrupole and shielding parameters with those computed from the active site model, the agreement between theory and experiment providing a metric for the quality of the model. Hence, the combination of X-ray diffraction, low-temperature solid-state NMR spectroscopy, and molecular theory can be utilized to develop a testable model for the active site of metalloproteins (Table 2).

Acknowledgment. The authors want to acknowledge useful discussions with Professors Penner-Hahn and Fierke of the Department of Chemistry at the University of

(32) Warshel, A.; Levitt, M. *J. Mol. Biol.* **1976**, *103*, 227–249.
(33) Singh, U. C.; Kollman, P. A. *J. Comput. Chem.* **1986**, *7*, 718–730.
(34) Warshel, A. *Computer Modeling of Chemical Reactions in Enzymes and Solutions*; Wiley: New York, 1997.
(35) Gao, J. *In Reviews In Computational Chemistry*; Lipkowitz, K. B., Boyd, D. B., Eds.; VCH Publishers: New York, 1995; Vol. *7*, pp 119–185.

Michigan. This research was supported by the National Institutes of Health to PNNL (Federal Grant EB002050) and G.P. (GM046502). The NMR experiments were carried out in the Environmental Molecular Sciences Laboratory (a national scientific user facility sponsored by the Department of Energy Office of Biological and Environmental Research) located at Pacific Northwest National Laboratory and operated for DOE by Battelle. *NWChem* Version 5.0, as developed and distributed by Pacific Northwest National Laboratory, P.O. Box 999, Richland, WA 99352, and funded by the U.S. Department of Energy, was used to obtain some of these results.

Supporting Information Available: The coordinates from the geometry optimizations that utilized Ahlrich's double-ζ level (including polarization functions) basis set for **I** and **II** are given below. This material is available free of charge via the Internet at http://pubs.acs.org.

IC800009B